The Journal of Neuroscience, April 15, 2000, *20*(8):2994–3005

The Role of the Hyperpolarization-Activated Current in Modulating Rhythmic Activity in the Isolated Respiratory Network of Mice

Muriel Thoby-Brisson, Petra Telgkamp, and Jan-Marino Ramirez

Department of Organismal Biology and Anatomy, Committee on Neurobiology, The University of Chicago, Chicago, Illinois 60637

We examined the role of the hyperpolarization-activated current (I_h) in the generation of the respiratory rhythm using a spontaneously active brainstem slice of mice. This preparation contains the hypoglossus (XII) nucleus, which is activated in-phase with inspiration and the pre-Bötzinger complex (PBC), the presumed site for respiratory rhythm generation. Voltage-clamp recordings ($n = 90$) indicate that cesium (Cs) (5 mM) blocked 77.2% of the I_h current, and ZD 7288 (100 μM) blocked 85.8% of the I_h current. This blockade increased the respiratory frequency by 161% in Cs and by 150% in ZD 7288 and increased the amplitude of integrated population activity in the XII by 97% in Cs and by 162% in ZD 7288, but not in the PBC (Cs, by 19%; ZD 7288, by −4.56%). All inspiratory PBC neurons ($n = 44$) recorded in current clamp within the active network revealed a significantly decreased frequency of action potentials during the interburst interval and an earlier onset of inspiratory bursts after I_h current blockade. However, hyperpolarizing current pulses evoked only in a small proportion of inspiratory neurons (0% of type I; 29% of type II neurons) a depolarizing sag. Most of the neurons expressing an I_h current (86%) were pacemaker neurons, which continued to generate rhythmic bursts after inactivating the respiratory network pharmacologically with CNQX alone or with CNQX, AP-5, strychnine, bicuculline, and carbenoxolone. Cs and ZD 7288 increased the frequency of pacemaker bursts and decreased the frequency of action potentials between pacemaker bursts. Our findings suggest that the I_h current plays an important role in modulating respiratory frequency, which is presumably mediated by pacemaker neurons.

Key words: I_h *current; cesium; ZD 7288; rhythm generation; brainstem; respiratory neurons; mammals; mouse*

Great progress has been made in understanding the voltage-dependent ion channels that are critical for generating rhythmic activity. One membrane conductance that plays a key role in rhythm generation is the hyperpolarization-activated inward current (I_h current). Activated during a phasic hyperpolarization, this mixed cation current induces a slow membrane depolarization (Pape, 1996). This property may therefore not only terminate a phasic hyperpolarization but also initiate a depolarization, which in turn activates other voltage-dependent currents. This sequence of events results in the termination of one and initiation of another cycle. Consequently, in many neural networks, blocking the I_h current with cesium (Cs) (DiFrancesco et al., 1986) or ZD 7288 (Gasparini and DiFrancesco, 1997; Lüthi et al., 1998) causes a disturbance of phase-switching mechanisms, which leads to a decrease in the frequency of rhythmic activity. The role of the I_h current has been described in several neural networks in vertebrates and invertebrates (Angstadt and Calabrese, 1989; McCormick and Pape, 1990; Golowasch and Marder, 1992; Lüthi and McCormick, 1998). Although this current is present in certain respiratory neurons (Berger et al., 1995; Rekling et al., 1996), its role in respiratory rhythm generation has not been investigated.

The respiratory rhythm is generated within the lower brainstem. A particularly important region is the pre-Bötzinger complex (PBC) (Smith et al., 1991; Schwarzacher et al., 1995). Lesioning the PBC *in vivo* abolishes breathing (Koshiya and Guyenet, 1998; Ramirez et al., 1998). Isolating the PBC in a slice preparation preserves rhythmic activity (Smith et al., 1991; Funk et al., 1994; Ramirez et al., 1996), which can be recorded either from the PBC or from the hypoglossal (XII) motor nucleus. The respiratory rhythm is characterized by three phases: inspiration, postinspiration, and active expiration (Richter, 1983). The generation of this three-phase rhythm depends on synaptic connectivity and membrane properties (Johnson et al., 1994; Smith et al., 1995; Ramirez et al., 1997). After the blockade of synaptic inhibition, rhythmic activity persists under *in vitro* conditions. Inspiratory neurons depolarize more rapidly but remain rhythmically active, whereas expiratory neurons become either tonic or discharge rhythmically in-phase with inspiration (Ramirez et al., 1997). Therefore, research efforts have focused on the neural mechanisms that lead to the generation of inspiratory activity. Inspiratory activity may be derived from pacemaker neurons (Johnson et al., 1994; Koshiya and Smith, 1999). According to a model proposed by Smith et al. (1995), rhythmic activity in individual pacemaker neurons is synchronized via glutamatergic mechanisms to form the inspiratory burst (Rekling and Feldman, 1998). Synaptic inhibition transforms this pacemaker-driven inspiratory activity into the three-phase respiratory rhythm.

However, the separation of a pacemaker-driven inspiratory rhythm and a synaptically driven transformation into the three-phase rhythm is artificial. Under control conditions, synaptic processes will affect pacemaker properties and vice versa. Thus, an inspiratory burst will be terminated by both intrinsic membrane properties and synaptic inhibition. Inhibitory mechanisms

Received Sept. 23, 1999; revised Feb. 3, 2000; accepted Feb. 3, 2000.

This study was supported by National Institutes of Health Grant HL60120/JMR.

Correspondence should be addressed to Dr. Jan-Marino Ramirez, Department of Organismal Biology and Anatomy, Committee on Neurobiology, The University of Chicago, 1027 East 57th Street, Chicago, IL 60637. E-mail: jramire@midway.uchicago.edu.

 0270-6474/00/202994-12$15.00/0

may also influence the formation of the inspiratory burst. In a model published by Ramirez and Richter (1996), synaptic inhibition activates the I_h current, which contributes to the next inspiratory burst. However, the role of the I_h current in this model was hypothetical and without experimental evidence. Therefore, we examined the possible contribution of the I_h current in generating inspiratory activity. Three types of inspiratory neurons have been identified previously (Rekling et al., 1996). One neuron type (type 3) is silent during the interburst interval. These neurons are presumably ambiguus motoneurons (Rekling et al., 1996) and will not be considered here. The two other types of inspiratory neurons (types 1 and 2) discharge before the inspiratory XII burst and will be considered in our study.

In this study, we evaluated the effect of blocking the I_h current on the electrical activity of type 1 and type 2 inspiratory neurons and on the population activity recorded from the PBC and XII. Contrary to our expectation, the blockade of the I_h current did not cause a decrease, but an increase in the respiratory frequency.

Parts of this paper have been published previously in abstract form (Thoby-Brisson et al., 1998, 1999).

MATERIALS AND METHODS

Preparation. Experiments were performed on male and female mice (7- to 22-d-old) that were deeply anesthetized with ether and decapitated at the C3–C4 level. The procedure to obtain functional brainstem slices has been described previously (Ramirez et al., 1996) and will be only briefly summarized here. The brainstem was isolated in an ice-cold artificial CSF (a-CSF) bubbled with carbogen (95% oxygen and 5% CO_2). a-CSF contained (in mM): 128 NaCl, 3 KCl, 1.5 $CaCl_2$, 1 $MgSO_4$, 24 NaHCO, 0.5 NaH_2PO_4, and 30 D-glucose and was equilibrated with carbogen at 29°C, pH 7.4. The brainstem was then glued onto an agar block with its rostral end up and mounted into a vibratome with the rostral end tilted at an ~20° angle to the plane of the razor blade. Thin slices were serially sectioned from rostral to caudal until the rostral boundary of the PBC became visible. This area was recognized by specific landmarks, such as the inferior olive, the nucleus ambiguus, and the XII nucleus (Fig. 1*A*). Slices that contained the PBC (500- to 600-μm-thick) were immediately transferred into a recording chamber and maintained at a temperature of 29°C. After the dissection, the preparation was stabilized for 30 min in a-CSF continuously perfused at a rate of 10 ml/min. The potassium concentration was raised from 3 to 8 mM over another 30 min to obtain spontaneous rhythmic activity, which was stable for up to 12 hr.

Recordings. Extracellular recordings were obtained with suction electrodes positioned either on the PBC or on the XII nucleus. The signal collected was amplified 2000 times and filtered (low-pass 1.5 kHz, high-pass 250 Hz). The signals were also rectified and integrated using an electronic filter (time constant of 30–50 msec). Intracellular patch-clamp recordings were obtained from both PBC neurons and hypoglossal neurons. These neurons were identified according to their anatomical location (Fig. 1*A*) and with respect to their discharge characteristics in relation to the population respiratory activity (Fig. 1*B*). We used two different techniques: the blind patch and the patch-clamp technique under visual control. The recordings were obtained using patch electrodes manufactured from borosilicate glass tubes containing a filament (Clarke GC150TF or GC120TF). Blind patch electrodes used for current-clamp recordings were filled with a solution containing (in mM): 140 K-gluconic acid, 1 $CaCl_2$*$6H_2O$, 10 EGTA, 2 $MgCl_2$*$6H_2O$, 4 Na_2ATP, and 10 HEPES. The K-gluconic acid containing electrode solution resulted in a significant liquid junctional potential (LJP) (>12 mV), which affected the measured membrane potentials. All membrane potential measurements were therefore compensated for this LJP as described by Neher (1992). Patch electrodes used for voltage-clamp recordings were filled with a solution containing (in mM): 140 KCl, 1 $CaCl_2$*$6H_2O$, 10 EGTA, 2 $MgCl_2$*$6H_2O$, 4 Na_2ATP, and 10 HEPES. This internal pipette solution resulted in small LJP (<3 mV), which was not corrected in this study. Neurons were held at a potential of either −40 or −60 mV. The I_h current was isolated by applying 2-sec-long step potentials from −40 to −140 mV. In some cases (as indicated in the figures), the currents were off-line leak subtracted by determining the leak with a single voltage step from −40 to −50 mV.

All recordings were stored with a personal computer on Axotape (Version 2.0) or pClamp6 (Axon Instruments, Foster City, CA). The stored files were analyzed off-line. Only recordings with good signal-to-noise ratios were quantitatively evaluated using software programs that were written with the commercially available program Igor Pro.

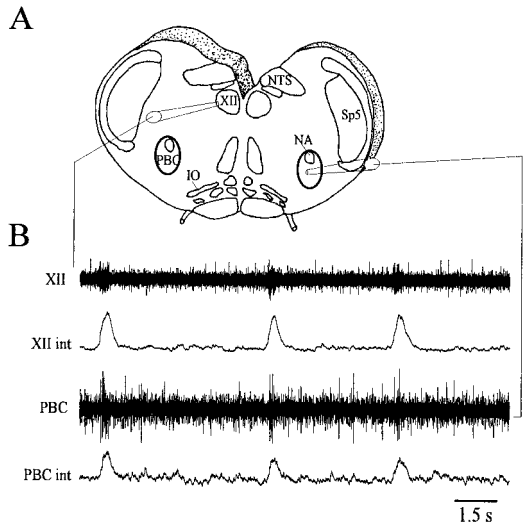

Figure 1. Experimental model and extracellular recording techniques. *A*, Scheme of a brainstem slice preparation obtained from mice. This slice contains the PBC, the XII nucleus, the inferior olive (*IO*), the nucleus ambiguus (*NA*), the nucleus tractus solitarius (*NTS*), and the spinal trigeminal nucleus (*Sp5*). *B*, Extracellular population recordings of respiratory activity from the XII (*top two traces*: *XII*, extracellular recording; *XII int*, integrated trace) and the PBC (*bottom two traces*: *PBC*, extracellular recording; *PBC int*, integrated trace).

Drugs were bath-applied at the final concentration of 2.5–5 mM cesium (Sigma, St. Louis, MO), 100 μM ZD 7288 (Tocris Cookson, Ballwin, MO), 3 mM barium (Sigma), 20 μM 6-cyano-7-nitroquinoxaline-2,3-dione (CNQX) (Tocris Cookson), 50 μM DL-2-amino-5-phosphonovaleric acid (AP-5) (Sigma), 5 μM strychnine (Sigma), 20 μM bicuculline (Sigma), and 50 μM carbenoxolone (CBX) (Sigma). None of these solutions caused a change in the LJP.

Statistical values are given as mean ± SEM value. Significance was assessed with the Student's *t* test, and values were assumed to be significant at $p < 0.05$.

RESULTS

Blockade of the I_h current with cesium and ZD 7288

The initial set of experiments was primarily performed to assess whether cesium and ZD 7288 are suitable agents to block the I_h current. Therefore, no attempt was made to functionally identify the PBC neurons under voltage-clamp conditions. This set of experiments is based on voltage-clamp recordings from 90 neurons identified according to the anatomical location of their soma. Thirty-eight percent of the neurons in the PBC ($n = 24$) and 73% of the neurons in the XII nucleus ($n = 66$) expressed a measurable I_h component (>50 pA at a voltage step of −100 mV). The I_h current was evoked by applying a series of hyperpolarizing voltage pulses incrementing in 10 mV steps from different holding potentials (either −40 or −60 mV) to −140 mV (Fig. 2*A*). However, this experimental protocol activated not only the I_h current but also instantaneous current. Thus, to isolate the I_h current, we subtracted the current amplitude measured at the end of a voltage step (steady-state current containing the I_h and the instantaneous current) from the current amplitude measured at the beginning of a pulse (containing only the instantaneous current). The amplitude of the isolated I_h current in XII neurons ($n = 5$; V_h, −40 mV) (Fig. 2*B*, *filled squares*) was not significantly

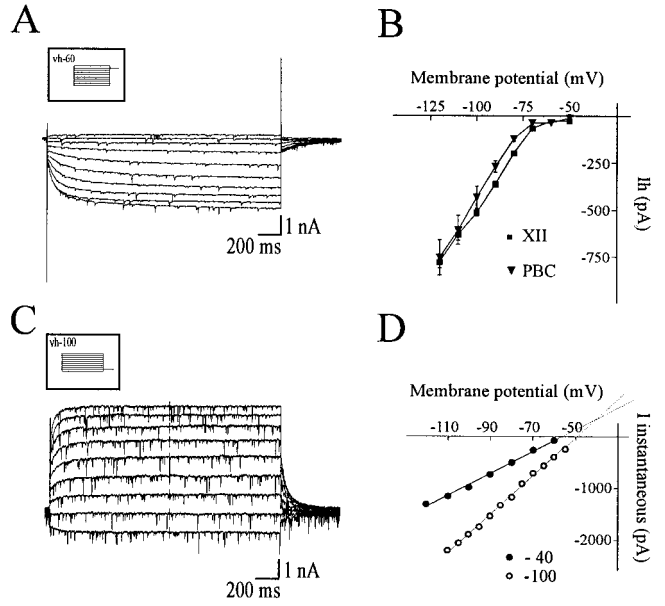

Figure 2. Characterization of the I_h current in PBC and XII neurons. *A*, Under voltage-clamp conditions, the I_h current slowly activates in response to hyperpolarizing voltage steps lasting for 2 sec. *B*, From a holding potential of −40 mV, the isolated I_h current shows similar amplitude values in XII ($n = 4$) and PBC ($n = 6$) neurons and begins to activate at −50 mV. *C*, *D*, The reversal potential can be extrapolated from the instantaneous currents of several voltage steps from the holding potential of −40 mV (no activation of I_h; *filled circles* in *D*) and from a holding potential of −100 mV (fully activated I_h; *open circles* in *D*; protocol and evoked currents at *C*).

different from the PBC neurons ($n = 6$; V_h, −40 mV) (Fig. 2*B*, *filled triangles*). The I_h current became first measurable at −50 mV. However, at this potential, the current was very small in both XII (26 ± 4 pA; $n = 5$; V_h, −40 mV) and PBC (10 ± 3 pA; $n = 4$; V_h, −40 mV) neurons. The reversal potential of the I_h current for XII and PBC neurons was between −20.3 and −41.4 mV ($n = 4$). This value was assessed by using the extrapolation method (Mayer and Westbrook, 1983; Takahashi, 1990; Bayliss et al., 1994). We plotted the instantaneous current elicited from a holding potential at which the I_h current was not activated (V_h, −40 mV) (Fig. 2*D*, *filled circles*) and the instantaneous current at a holding potential when the I_h current was fully activated (−100 mV) (Fig. 2*C*,*D*, *open circles*). The *I–V* plots of these instantaneous current (Fig. 2*D*) were fitted with linear regressions. In these plots, the increased conductance at −100 mV corresponded to the chord conductance of the I_h current, and the extrapolated intersection of the two regression lines corresponded to the reversal potential that was at −41.4 mV (Fig. 2*D*).

To evaluate the role of the I_h current in respiratory rhythm generation, it was essential to selectively block this current. Therefore, we compared the differential effect of cesium, barium, and ZD 7288 on the I_h current and on the instantaneous current (Fig. 3). The instantaneous current was presumably caused by two currents: an inward rectifier current and a leak current. A differential effect on these two instantaneous currents is shown on Figure 3. The *top panel* (Fig. 3*A*) shows the hyperpolarization activated currents, including the leak current; the *bottom panel* (Fig. 3*B*) shows the currents after the subtraction of the leak current (off-line leak subtraction). The instantaneous current was reduced by cesium and barium (Fig. $3A_1$,A_2). In contrast, ZD 7288 had no effect on the instantaneous current as shown for an example with a rather large instantaneous current (Fig. $3A_3$). The instantaneous current, which was evoked even after leak subtraction, was presumably caused by the inward rectifier current (Fig. 3*B*). This remaining instantaneous current was blocked by cesium (Fig. $3B_1$) and by barium (Fig. $3B_2$). This barium sensitivity is further indicative for the inward rectifier current. In contrast to barium and cesium, ZD 7288 blocked only the I_h current but did not affect the leak current (Fig. $3A_3$) or the inward rectifier (Fig. $3B_3$).

Because bath application of both cesium and ZD 7288 led to a reduction of the I_h current (Fig. $3A_1$,B_1,A_3,B_3), we further characterized their efficacy to block this current. The I_h current amplitude was diminished by cesium (Fig. 4*A*, *open symbols*) and ZD 7288 (Fig. 4*B*, *open symbols*) at all membrane potentials more negative than −60 mV. ZD 7288 (100 μM) blocked 85.8 ± 6.12% (i.e., 14% of control current amplitude left) of the I_h current evoked by voltage steps from −60 to −120 mV ($n = 5$) (Fig. 4*C*, *black bar*). Bath application of cesium (2.5–5 mM) blocked under the same experimental conditions the I_h current by 77.28 ± 6.05% (i.e., 22.7% of control current amplitude left; at 2.5 mM Cs, to 24.02 ± 13.07%; $n = 3$; at 5 mM Cs, to 21.74 ± 6.48%; $n = 4$) (Fig. 4*C*, *gray bar*).

It is well established that cesium inhibits at higher concentrations not only the I_h current but also potassium outward currents. Thus, it was important to assess the possible inhibitory effect of 5 mM cesium on potassium outward currents. PBC neurons were voltage clamped at a holding potential of −70 mV, and hyperpolarizing and depolarizing potentials were applied in 10 mV steps from −80 to +40 mV (Fig. 4*D*) in the presence or absence of cesium. As illustrated in the original *traces* of Figure 4*D*, the inhibitory effect of cesium on these currents was very weak (compare *right* and *left panels*). The *I–V* curve in Figure 4*E*, obtained by measuring the potassium current amplitude at the end of the pulse (steady state, $n = 4$), shows that the blockade of potassium currents with 5 mM cesium was weak and only significant at a very positive voltage (+40 mV) (Fig. 4*E*).

Effect of I_h current blockade on the respiratory network activity

The effect of blocking the I_h current on respiratory network activity was assessed by recording simultaneously population activity from the presumed respiratory rhythm generator (PBC) and its motor output in the XII nucleus (Fig. 5). For this purpose, extracellular electrodes were positioned onto the surface of the PBC and/or the XII nucleus. In 27 preparations, bath application of cesium had two major effects on the extracellularly recorded and integrated population activity (Fig. 5*A*): (1) there was an increase in respiratory frequency, and (2) there was an increase in the amplitude of the integrated population activity in the hypoglossal nucleus but not in the PBC.

These changes were quantitatively analyzed for 15 recordings from the PBC and 14 recordings from the XII nucleus (Fig. 5*A*, *graph*). In all examined preparations, respiratory burst activity occurred synchronously in the PBC and XII nucleus, indicating that rhythmic activity within the XII was dominated by inspiratory activity. Consequently, the frequencies measured in different slices independently in the XII and PBC were not statistically different and were thus combined. After the blockade of the I_h current with 5 mM cesium, the frequency was significantly increased by 160.8 ± 16.29% ($n = 27$). This effect caused a more than twofold increase in the average respiratory frequency from 0.22 Hz under control conditions to 0.48 Hz in the presence of

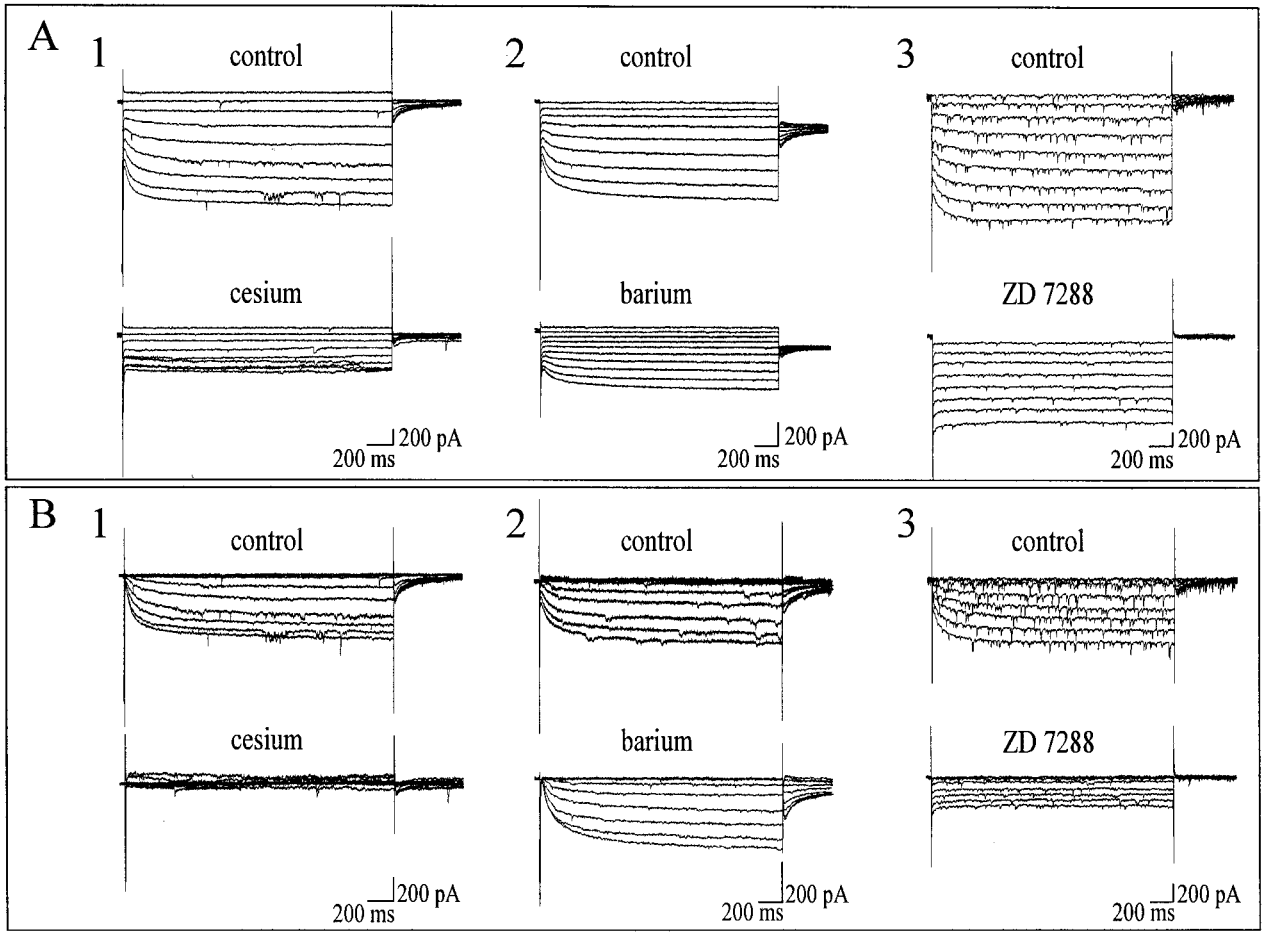

Figure 3. Hyperpolarization-activated currents are differentially blocked by cesium (*1*), barium (*2*), and ZD 7288 (*3*). *A* and *B* show currents evoked by hyperpolarizing voltage steps applied from a holding potential of −60 mV (except for A_3 and B_3: V_h, −40 mV). *A* shows currents before leak subtraction. *B* shows currents after off-line leak subtraction. *Top traces*, Currents evoked under control conditions. *Bottom traces*, Current responses of the same neurons to the same protocols in the presence of 2.5 mM cesium chloride (*A*), 3 mM barium (*B*), and 100 μM ZD 7288. Note that cesium blocked the slow activating I_h and instantaneous currents, barium reduced only the instantaneous current, and ZD 7288 blocked only the slow activating I_h current.

cesium. The integrated burst amplitude increased significantly in the XII nucleus (96.6 ± 22.2%; $n = 14$) but not in the PBC (18.7 ± 3.96%; $n = 15$).

The alterations of respiratory activity induced by perfusion of 100 μM ZD 7288 (Fig. 5*B*) were similar to those described for cesium. Qualitatively, the blockade of the I_h current with ZD 7288 induced also (1) an increase in respiratory frequency and (2) a significant increase in the XII amplitude. Quantitatively (Fig. 5*B*, *graph*), the respiratory frequency increased on average by 150 ± 30% ($n = 19$), and the amplitude in the hypoglossal activity increased by 162 ± 9.72% ($n = 5$). The amplitude was not significantly affected in the PBC (−4.56 ± 6.23%; $n = 15$). The effects obtained in the presence of ZD 7288 were not significantly different from those obtained in the presence of cesium.

Are the effects of the I_h current blockade dependent on the excitability of the respiratory network?

Using model cells, it has been shown that the effects of the I_h current on the frequency depend on the excitability state of the rhythm generating network (Sharp et al., 1996). This has also been demonstrated for real neurons in the inferior olive network (Bal and McCormick, 1997). In the slices examined in our study, the spontaneous frequency of the respiratory rhythm varied under control conditions from 0.07 to 0.35 Hz. This variability in the excitability state of the network might affect the modulatory effect of the I_h current. Therefore, we examined whether the effect of I_h current blockade with cesium was dependent on the initial frequency of the respiratory rhythm. In Figure 6*A* (*filled squares*), the respiratory frequency was plotted in the presence of cesium versus the initial frequency recorded under control conditions. These measurements revealed that blockade of the I_h current induced an increase in the respiratory frequency at all examined frequencies. However, the effect of cesium was more pronounced at lower initial frequencies. For frequencies below 0.1 Hz, the blockade of the I_h current induced on average a change of 178%, whereas for higher frequencies (greater than 0.15 Hz), the changes were on average no more than 100%.

As described in Materials and Methods, the network excitability was routinely increased by raising the concentration of K^+ from 3 to 8 mM. In this set of experiments (Fig. 6*B*), the excitability of the network was decreased by lowering the concentration of extracellular K^+ from 8 to 3 mM. Under these conditions, transverse slices expressed no rhythmic activity (Fig. 6*B*, *left* part of the recording). In eight of nine preparations, bath application of cesium induced rhythmic activity (Fig. 6*B*, *right* part of the

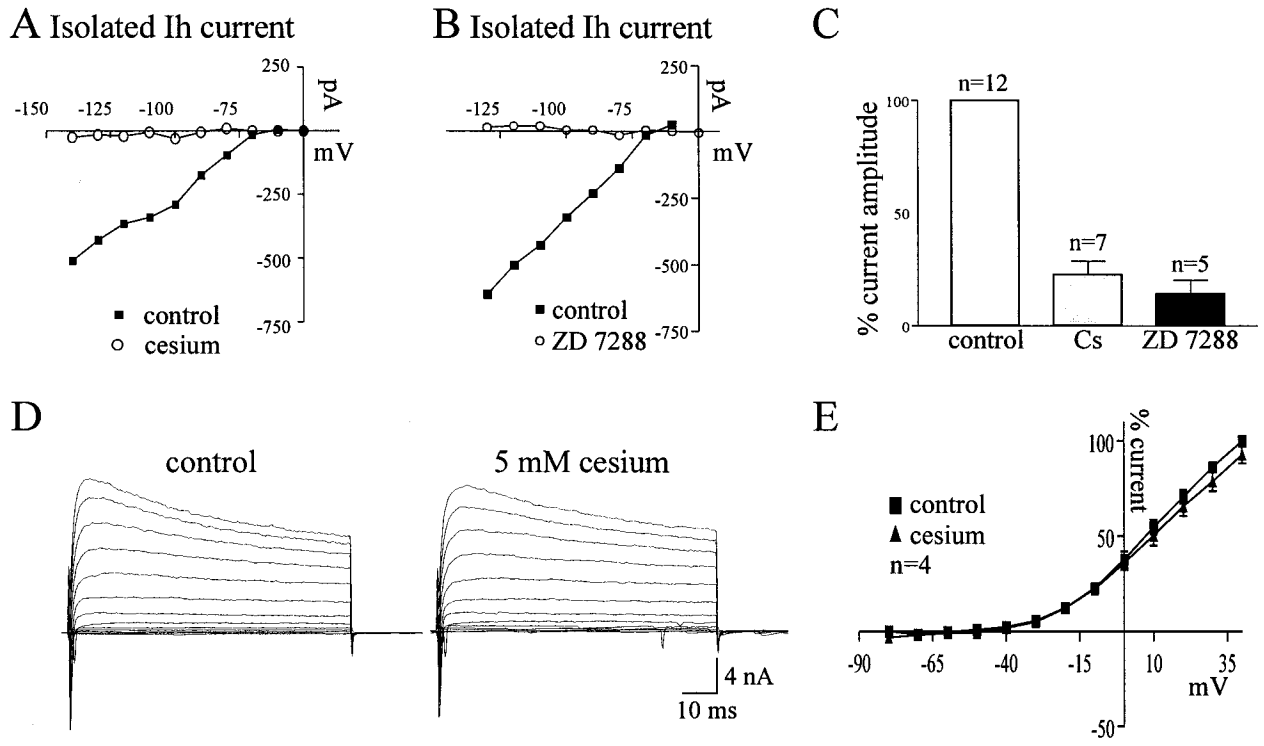

Figure 4. Cesium (*A*) and ZD 7288 (*B*) are potent blockers of the I_h current amplitude. *A*, *B*, Amplitude of the I_h current is plotted against the membrane potential under control conditions (*filled squares*) and after bath application of cesium (*A*, *open circles*) or ZD 7288 (*B*, *open circles*). All voltage steps were applied from a holding potential of −60 mV. *C*, Histogram showing the percentage of the I_h current that remained unblocked during bath application of cesium (*middle gray bar*) or ZD 7288 (*black bar*). The values were determined from voltage steps from a holding potential of −40 mV to a potential of −120 mV. The numbers of slices used for these experiments are indicated on each bar. The control bar summarizes all experiments for cesium and ZD 7288. *D*, *E*, Effect of 5 mM cesium on potassium outward currents recorded in respiratory neurons. *D*, Hyperpolarizing and depolarizing potentials were applied in 10 mV steps from −80 to +40 mV in control conditions (*left*) and under cesium (*right*). The holding potential was −70 mV. *E*, The *I–V* curve is based on four recordings from respiratory neurons using the same protocol as described in *D*. The potassium current amplitude was obtained at the end of the pulse (steady state) and normalized to the maximal amplitude under control conditions (100%).

recording), which remained stable as long as the cesium was present in the bath. Similar results were obtained for four of five preparations treated with ZD 7288. These results further indicated that the I_h current had an inhibitory action on the respiratory network activity, which contributes in these *in vitro* preparations to the cessation of rhythmic activity in the presence of 3 mM K^+.

In two preparations, we enhanced the network excitability by raising the concentration of K^+ from 8 to 10 mM. Under these conditions the "control" respiratory frequency of more than 0.5 Hz was further enhanced in the presence of cesium. The average frequency of these experiments was added as *open circles* in Figure 6*A*.

Effect of I_h current blockade on the electrical activity of type 1 inspiratory neurons

Three types of inspiratory neurons were characterized by Rekling et al. (1996). Two of these neurons (types 1 and 2) discharge before the inspiratory XII burst and may therefore contribute to the initiation of inspiration (Rekling et al., 1996). As shown in Figure 7, *A* and *B* (*top traces*), type 1 neurons generated several brief bursts of action potentials that preceded the generation of an inspiratory burst. These neurons exhibited no tonic activity during the interburst interval. To examine whether type 1 neurons possess an I_h current, it was necessary to identify the depolarization pattern in the active network and then abolish respiratory network activity by blocking glutamatergic synaptic transmission with CNQX (20 μM). In the absence of synaptic membrane fluctuations, hyperpolarizing current pulses injected into five type 1 neurons evoked no depolarizing sags (Fig. 7*C*), confirming the conclusions of Rekling et al. (1996), that type 1 neurons exhibit no I_h current.

However, in the active network, the discharge pattern of type 1 neurons was altered by blocking the I_h current. Application of cesium (Fig. 7*A*, *bottom traces*) or ZD 7288 (Fig. 7*B*, *bottom traces*) increased the respiratory frequency and decreased the occurrence of brief bursts generated between two inspiratory bursts. The interburst frequency of action potentials was reduced from 3.05 ± 0.72 Hz under control conditions to 0.54 ± 0.35 Hz after the I_h current blockade ($n = 4$) (Fig. 7*D*, interburst frequency). These average values were obtained by evaluating in each preparation the number of action potentials generated during 15 consecutive interburst intervals. The number of action potentials was divided by the duration of the interburst interval to obtain the average action potential frequency. Neither the burst duration (0.94 ± 0.19 sec in control conditions and 0.98 ± 0.11 sec under cesium; $n = 5$) (Fig. 7*D*) nor the intraburst frequency (29.69 ± 7.7 Hz in control conditions and 29.97 ± 5.96 Hz under cesium; $n = 4$) (Fig. 7*D*) was significantly affected by the blockade of the I_h current. The membrane potential of these neurons was also not significantly altered by the application of I_h blockers (from −63.25 ± 1.03 mV under control to −62.5 ± 1.75 mV after blockade of the I_h current; $n = 5$). Because type 1 neurons exhibited no I_h current (Fig. 7*C*), we assume that the alterations

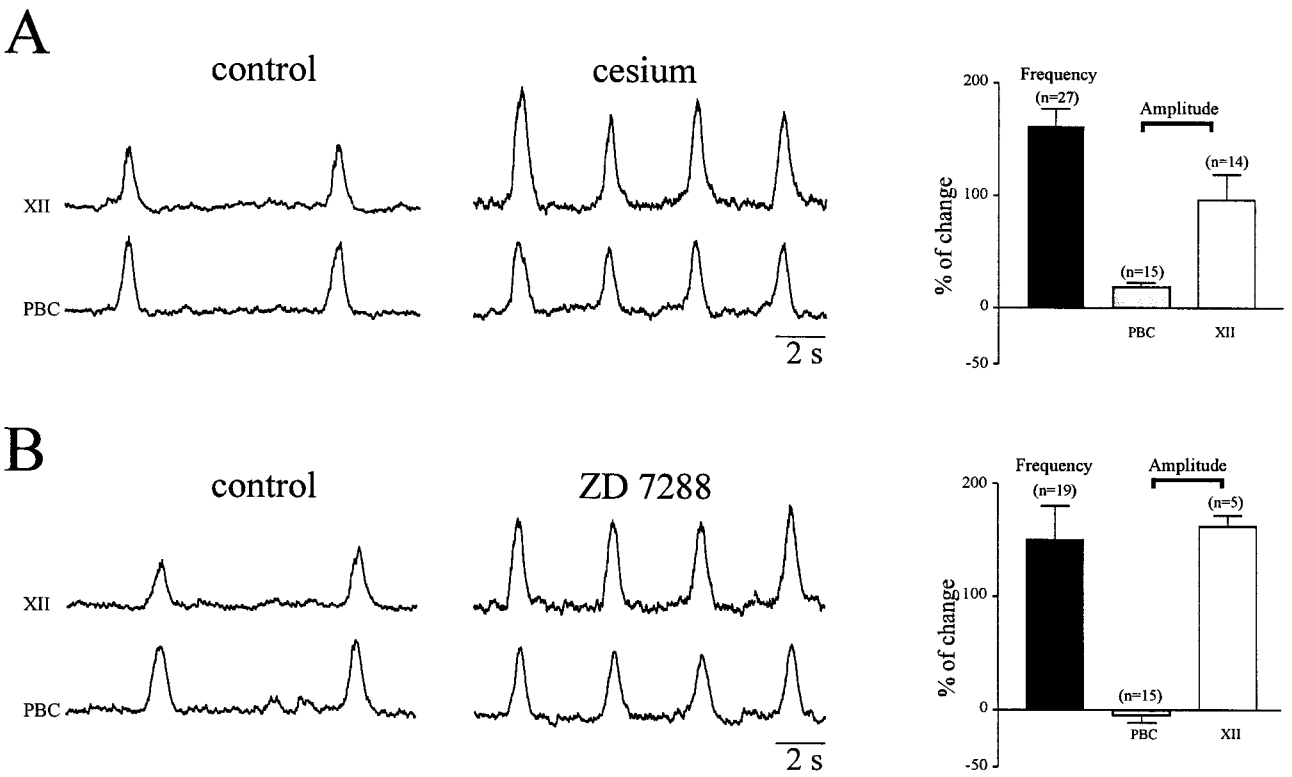

Figure 5. Changes induced in respiratory activity after the blockade of the I_h current with cesium (*A*) and ZD 7288 (*B*). *A*, Integrated recordings of respiratory activity obtained simultaneously from the XII nucleus (*top trace*) and the PBC (*bottom trace*) under control conditions (*left*) and in the presence of 5 mM cesium (*right*). Bar histograms representing the cesium-induced change (percentage) in the frequency (*black bar*) and the amplitude of integrated respiratory activity recorded in the PBC (*gray bar*) and the XII nucleus (*white bar*). *B*, Same as described in *A*, except that I_h was blocked by 100 μM ZD 7288 instead of 5 mM cesium. The numbers of slices used for these experiments are indicated on each bar.

in the discharge pattern were synaptically mediated and not attributable to a direct effect of Cs or ZD 7288 on type 1 neurons.

Effect of I_h current blockade on the electrical activity of type 2 inspiratory neurons

In contrast to type 1 neurons, type 2 neurons exhibit under control conditions tonic activity during the interburst interval and no brief bursts of action potentials (Rekling et al., 1996) (Figs. 8*A*,*B*, *top traces*, 9*A*,*B*, *top traces*). To examine the presence of the I_h current in type 2 neurons, we identified 31 type 2 neurons in the active network before eliminating network activity with CNQX (20 μM). Twenty-two type 2 neurons exhibited no depolarizing sag (Fig. 8*A*) in response to hyperpolarizing current injections. However, in nine type 2 neurons, a slow depolarization developed in response to negative current injections, which is indicative of the presence of an I_h current (Fig. 8*B*).

In the active network, application of cesium (Fig. 9*A*, *bottom traces*) or ZD 7288 (Fig. 9*B*, *bottom traces*) altered the discharge pattern of all type 2 neurons, irrespective of the presence or absence of an I_h current. The respiratory frequency increased in response to both blockers, and the frequency of action potentials generated between two inspiratory bursts decreased from 3.50 ± 0.72 Hz under control conditions to 0.10 ± 0.08 Hz after the I_h current blockade ($n = 8$) (Fig. 9*C*, interburst frequency). These average values were obtained as described above for type 1 neurons. Blockade of the I_h current affected only the interburst interval. There was no significant change in the intraburst frequency (26.39 ± 4.15 Hz under control conditions and 27.01 ± 3.18 Hz after the I_h current blockade; $n = 8$) (Fig. 9*C*) and no change in the inspiratory burst duration (0.89 ± 0.11 sec under control conditions and 1.07 ± 0.11 sec after the I_h current blockade; $n = 8$) (Fig. 9*C*). Blockade of the I_h current did not alter significantly the membrane potential of type 2 neurons (from −62.5 ± 2.83 mV under control to −61.67 ± 2.14 mV in the presence of I_h blockers; $n = 8$).

The I_h current is more often expressed in type 2 pacemaker neurons compared with type 2 follower neurons

As demonstrated by Koshiya and Smith (1999), a population of neurons maintains rhythmic activity after the elimination of respiratory network activity with CNQX. These neurons are considered to be pacemaker neurons (Koshiya and Smith, 1999). To examine whether the presence of the I_h current in type 2 neurons was linked to such pacemaker properties, we identified 25 type 2 neurons in the active network and then recorded their activity after the blockade of respiratory network activity in the presence of CNQX (20 μM). Most neurons ($n = 18$) became tonically active after the elimination of respiratory network activity (Fig. 10A_2) and are therefore considered to be follower neurons. Only 36% of these neurons expressed an I_h current (3 of 18 recorded type 2 follower neurons) (Fig. 10*C*). Seventeen of these follower neurons (Fig. 10A_3) remained tonically active in the presence of either cesium or ZD 7288. However, in 1 of the 18 neurons, cesium application induced rhythmic bursting. This follower neuron exhibited an I_h current. However, because this phenomenon was only observed once, its significance cannot be assessed.

Seven of 25 type 2 neurons remained rhythmically active after

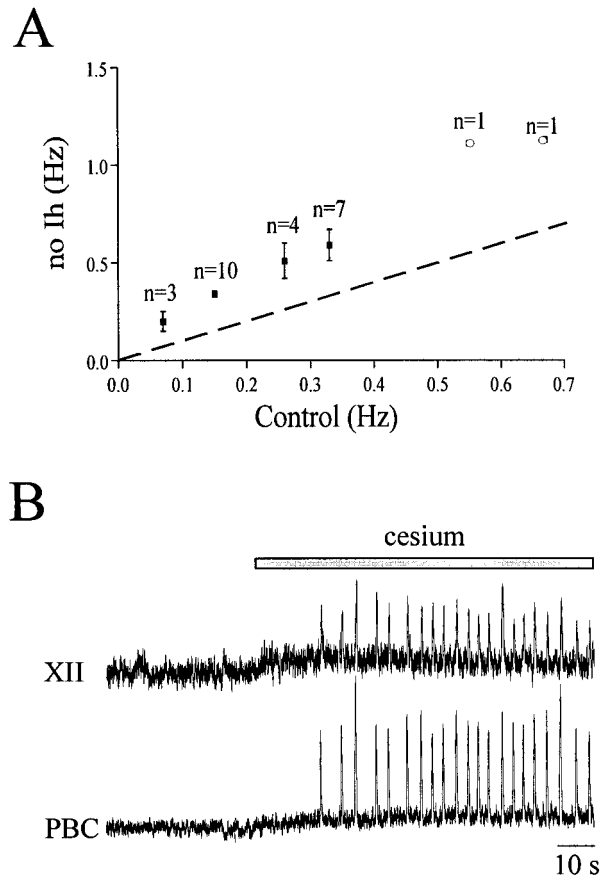

Figure 6. Cesium-induced effects at different excitability states of the respiratory network. *A*, Graph indicating the respiratory frequency after blockade of the I_h current with cesium (ordinate) versus the respiratory frequency before the I_h current blockade obtained in an a-CSF containing 8 mM K^+ (*filled circles*) or 10 mM K^+ (*open circles*) (abscissa). *Numbers* indicate the number of experiments performed at each frequency. *B*, Effect of cesium on the respiratory network, which was inactive in the presence of an a-CSF containing 3 mM K^+ (*left* part of the recording). Rhythmic activity appeared at a concentration of 3 mM K^+ after the blockade of the I_h current with cesium (*right* part of the recording). The *gray box* corresponds to the time of cesium exposure.

blockade of glutamatergic connections and are therefore considered to be pacemaker neurons (Fig. $10B_2$). The discharge pattern of these neurons was not qualitatively altered in the presence of CNQX (Fig. 10, compare B_1 and B_2; see also *B*, *black bar*). Despite the absence of rhythmic population activity (Fig. $10B_2$, *extracellular trace*), these neurons generated rhythmic bursts and were tonically active during the interburst interval (Fig. $10B_1$,B_2). Hyperpolarizing current injections as described above revealed that the majority of the pacemaker neurons (86%; six of seven recorded type 2 pacemaker neurons) expressed an I_h current (Fig. 10*C*). This suggests that the I_h current may play an important role in the generation of respiratory pacemaker activity.

Application of cesium or ZD 7288 increased the bursting frequency in all examined pacemaker neurons except for the one neuron, which exhibited no I_h current (the average increase for all neurons was 188%) (compare Fig. $10B_3$ with $10B_2$, *white bar* in the graph). The frequency of action potentials generated during the interburst interval decreased from 8.19 ± 0.67 Hz under control conditions to 0.00 Hz (no action potential) after the blockade of the I_h current. These alterations resemble those observed in the intact network. Similar to the observations in the intact network, the membrane potential value of pacemaker neurons was also not altered after the application of cesium or ZD 7288 (from −62.33 ± 3.16 mV under control to −62.5 ± 3.78 mV in the presence of I_h blockers; $n = 7$).

The absence of a significant alteration in the membrane potential after the I_h current blockade was unexpected and raised the question whether these pacemaker neurons were sufficiently isolated from the network to exclude possible network effects. We tested a group of five pacemaker neurons by synaptically isolating these neurons not only with CNQX (20 μM) but also by applying AP-5 (50 μM) to block NMDA-mediated synaptic transmission, high concentrations of strychnine (5 μM) to block glycinergic and partially also GABAergic synaptic transmission, and also CBX (50 μM) to block possible electrical coupling. In three examples, we applied also bicuculline (20 μM) to block GABAergic synaptic transmission. All pacemaker neurons remained rhythmically active under these conditions (Fig. $11B_1$,D_3). The order with which these blockers were applied was random, and two examples are shown in Figure 11. The rhythmic activity persisted in the presence of AP-5, strychnine, CNQX, and CBX, and the frequency of rhythmic bursting was increased in the presence of ZD 7288 (Fig. $11B_2$). The frequency of rhythmic bursting in CNQX was increased in the presence of cesium (Fig. $11D_2$), and the rhythmic bursting persisted in the presence of strychnine, AP-5, CBX, and bicuculline. Note that there was an increase in the duration of the rhythmic bursts after the application of bicuculline, which may be attributable to an additional effect on calcium-dependent potassium channels. The persistence of rhythmic activity in all examined neurons suggests that the rhythmicity is generated intrinsically and is not dependent on the presence of a rhythmic synaptic input.

Another indication that the rhythmicity in these neurons was independent of synaptic input came from current injections. In all examined pacemaker neurons, additional bursts could be elicited in the intact network. These additional bursts were independent from synaptic input and could be elicited by either positive current injections (Fig. $11A_2$) or releasing these neurons from negative current injections (Fig. $11C_2$).

DISCUSSION

In this study, we have demonstrated that blockade of the I_h current caused a significant increase in the respiratory frequency and an augmentation in the amplitude of integrated XII bursts. Intracellular recordings from type 1 and type 2 inspiratory neurons indicated that blockade of the I_h current modulates the bursting frequency and the interburst frequency of action potentials without affecting the intraburst frequency or the burst duration. Current injections demonstrated that the majority of pacemaker type 2 neurons expressed an I_h current, suggesting that these neurons were responsible for the I_h-dependent modulation of the respiratory rhythm. Our conclusions are based on a comparison of rhythmic activity in the presence and absence of two I_h channel blockers: cesium and ZD 7288.

The specificity of the I_h current blockade

Cesium blocks not only the I_h current but also potassium currents (Spigelman and Puil, 1989; Coggan et al., 1994; Lin et al., 1996; Lotshaw, 1997). A diminution of potassium outward currents could explain an increase in the respiratory frequency caused by a general depolarization of neurons. However, this explanation is unlikely, because potassium outward currents were less sensitive

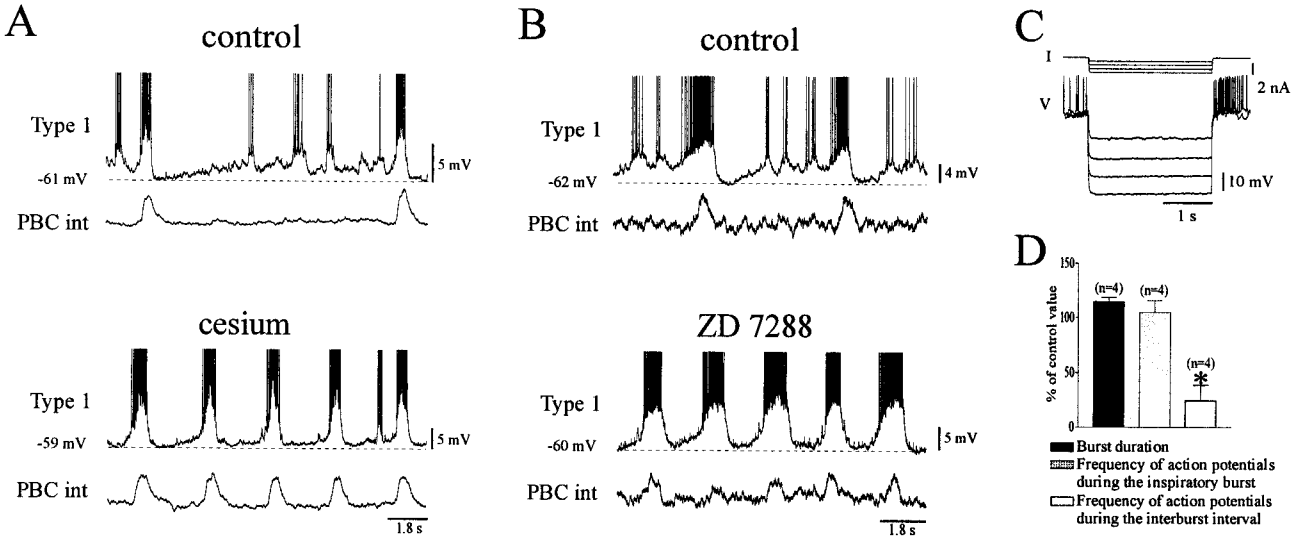

Figure 7. Effect of the I_h current blockade on the discharge pattern of type 1 inspiratory neurons. Intracellular recordings of type 1 neurons (*A*, *B*, *top traces*) recorded simultaneously with integrated activity in the PBC (*A*, *B*, *bottom traces*). The bursting frequency increases in the presence of 5 mM cesium and 100 μM ZD 7288. The frequency of action potentials occurring during the interburst interval is greatly reduced (*A*, *B*, *bottom panels*) compared with control conditions (*A*, *B*, *top panels*). *C*, Voltage responses (*bottom traces*) to negative current injections (scheme, 0.4 nA steps) into a type 1 neuron. Note that the hyperpolarizing current injections evoke no depolarizing sag. *D*, Bar histograms indicating the effect of blocking the I_h current on the burst duration (*black bar*), intraburst action potential frequency (*gray bar*), and interburst action potential frequency (*white bar*). The data were obtained from four recordings and are expressed as percentage of the control value. The *asterisk* indicates a statistically significant difference.

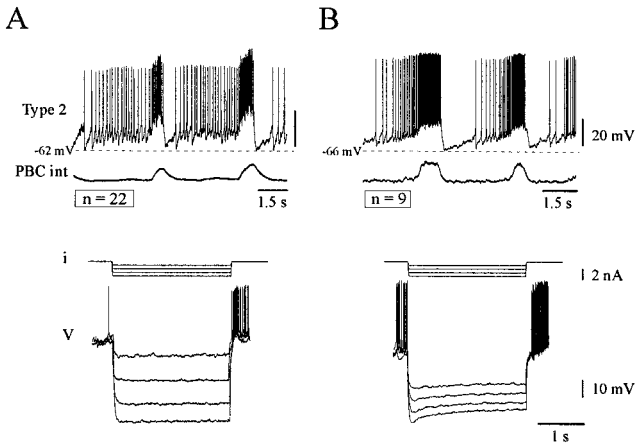

Figure 8. The I_h current is present in only a small proportion of type 2 inspiratory neurons. *A*, *B*, *Top*, Type 2 inspiratory neurons recorded simultaneously with integrated activity in the PBC. *Bottom*, Voltage responses (*bottom traces*) to negative current injections (scheme, 0.4 nA steps) of type 2 neurons in the presence of CNQX (20 μM). Sixty-six percent of the neurons ($n = 22$) developed no sag (*A*) and 34% of the neurons ($n = 9$) showed a depolarizing sag (*B*).

to cesium than the I_h current. A concentration of 5 mM blocked 77% of the I_h current, but only a small percentage of the potassium current that was only significant at "unphysiological" voltages more positive than +40 mV.

Alternatively, cesium may have blocked also inward rectifying currents (Wischmeyer and Karshin, 1997). These currents have a similar sensitivity to cesium as the I_h current, and they could also lead to a hyperpolarization-activated depolarization. However, it is unlikely that these currents contributed to the effects as observed in this study. The inward rectifier produces inward currents at potentials more negative than the potassium reversal potential (approximately −80 mV). Furthermore, we demonstrated that ZD 7288 (Harris and Constanti, 1995; Maccaferri and McBain, 1996) had effects similar to cesium. Because ZD 7288 had neither an effect on the inward rectifier nor an effect on the leak current, we assume that the effects described in this study were primarily attributable to the blockade of the I_h current.

Role of the I_h current in inspiratory neurons

Because blockade of the I_h current did not abolish respiratory rhythm generation, the rhythm-generating mechanism must be independent from the I_h current. Therefore, the data indicate that the I_h current has a modulatory role. The type 2 pacemaker neurons are possible candidates for this modulatory function. These neurons possessed an I_h current, and blockade of the I_h current induced changes in pacemaker activity that were strikingly similar to those observed in the intact neuronal network. However, blockade of the I_h current did not cause a significant shift in the membrane potential of these neurons. Thus, it remains unknown how the I_h current modulates these pacemaker properties. The I_h current could act as a leak current, which would affect the action potential generation without a measurable membrane depolarization. This would be consistent with the demonstration that the number of action potentials generated during the interburst interval decreased significantly despite the absence of a membrane potential shift. An alternative explanation is that the I_h current affected bursting properties primarily in dendritic processes, which were distant to the somatic recording. Dendritic currents could affect bursting properties without a measurable membrane potential shift in the soma. Furthermore, the dendritic processes may be more hyperpolarized than the soma, which could explain how the I_h current could have such a strong influence on the bursting properties.

Possible mechanisms how the I_h current slows down rhythmic activity have been described previously. In the thalamus and the inferior olive, the membrane potential can reach at low and intermediate levels of the I_h current a threshold that promotes pacemaker activity. However, at high levels of the I_h current, the

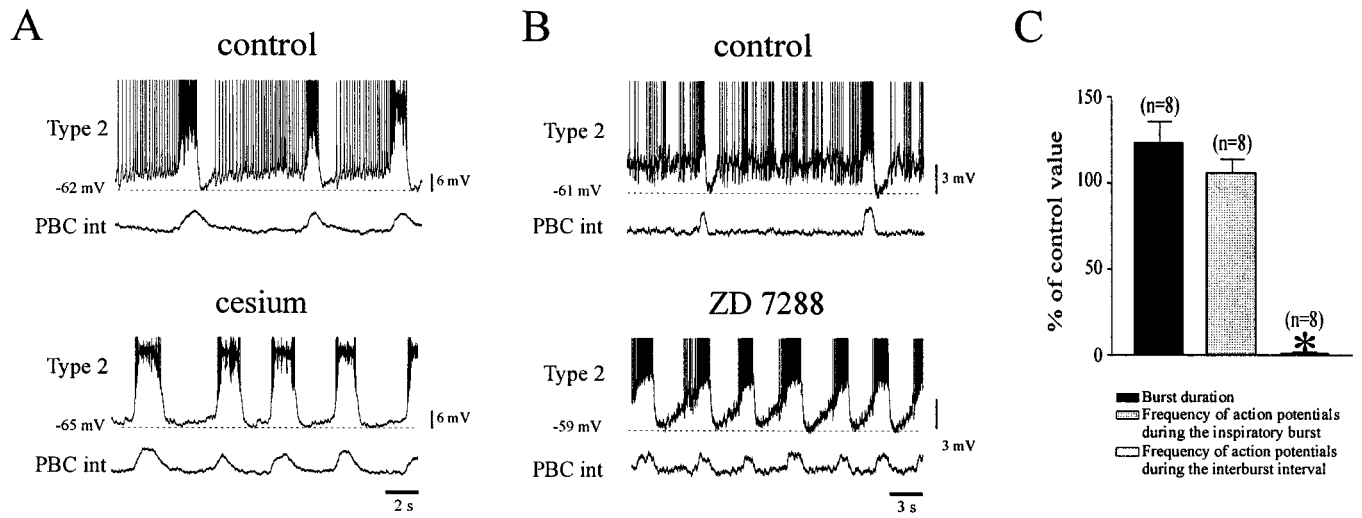

Figure 9. Effect of I_h current blockade on the discharge pattern of type 2 inspiratory neurons. Intracellular recordings of type 2 neurons (*A*, *B*, *top traces*) recorded simultaneously with integrated activity in the PBC (*A*, *B*, *bottom traces*). In the presence of 5 mM cesium (*A*) and 100 μM ZD 7288 (*B*), the bursting frequency increased and action potentials occurring during the interburst interval were greatly reduced (*A*, *B*, *bottom panels*) compared with control conditions (*A*, *B*, *top panels*). *C*, Bar histograms indicating the effect of blocking the I_h current on the burst duration (*black bar*), intraburst action potential frequency (*gray bar*), and interburst action potential frequency (*white bar*). The data were obtained from eight recordings and are expressed as percentage of the control value. The *asterisk* indicates a statistically significant difference.

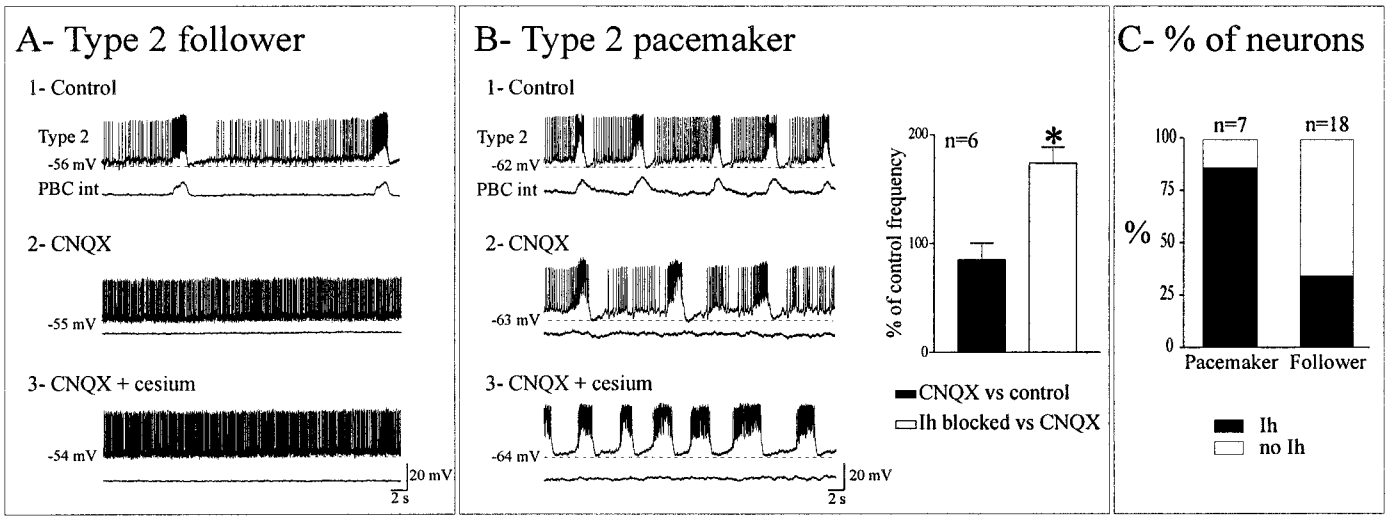

Figure 10. Effects of I_h current blockade on the activity of follower and pacemaker type 2 neurons after pharmacological elimination of respiratory network activity. *A*, Intracellular recording of a follower type 2 neuron (*top traces*) recorded simultaneously with integrated activity in the PBC (*bottom traces*) under control conditions (*1*), in 20 μM CNQX (*2*), and in 20 μM CNQX plus 5 mM cesium (*3*). *B*, *Left*, Same experimental procedure as described in *A* applied to a pacemaker type 2 neuron. *Right*, Bar histogram indicating the effect of CNQX (*black bar*) and CNQX plus I_h blockers (cesium, $n = 4$; ZD 7288, $n = 2$; *white bar*) on the bursting frequency of pacemaker neurons. The data are expressed as percentage of control value. The *asterisk* indicates a statistically significant difference. *C*, Percentage of type 2 follower ($n = 18$) and pacemaker ($n = 7$) neurons that express the I_h current.

membrane depolarization can cause the inactivation of these properties and neurons become tonically active (McCormick and Pape, 1990; Soltesz et al., 1991; McCormick and Bal, 1997). At this depolarized level, the network will be silent (Bal and McCormick, 1997). However, it is not very obvious how this mechanism could explain the findings within the respiratory network. In the respiratory network, it was possible to increase considerably the extracellular potassium concentrations (11 mM) without blocking rhythmic activity. Moreover, at these high concentrations of 11 mM potassium, blockade of the I_h current was still capable of further increasing the frequency of respiratory rhythmic activity. Thus, further experiments, possibly involving a combined computational and intracellular analysis of isolated respiratory pacemaker neurons, will be necessary to examine the mechanisms that lead to the I_h current-induced modulation of respiratory activity.

A possible physiological role for the I_h current in modulating respiratory activity

Although the underlying mechanisms remain hypothetical, it is clear that the I_h current can play an important role in regulating the frequency of the respiratory rhythm. The effect of blocking the I_h current has striking similarities with the initial phase of the respiratory response to hypoxia, the so-called augmentation

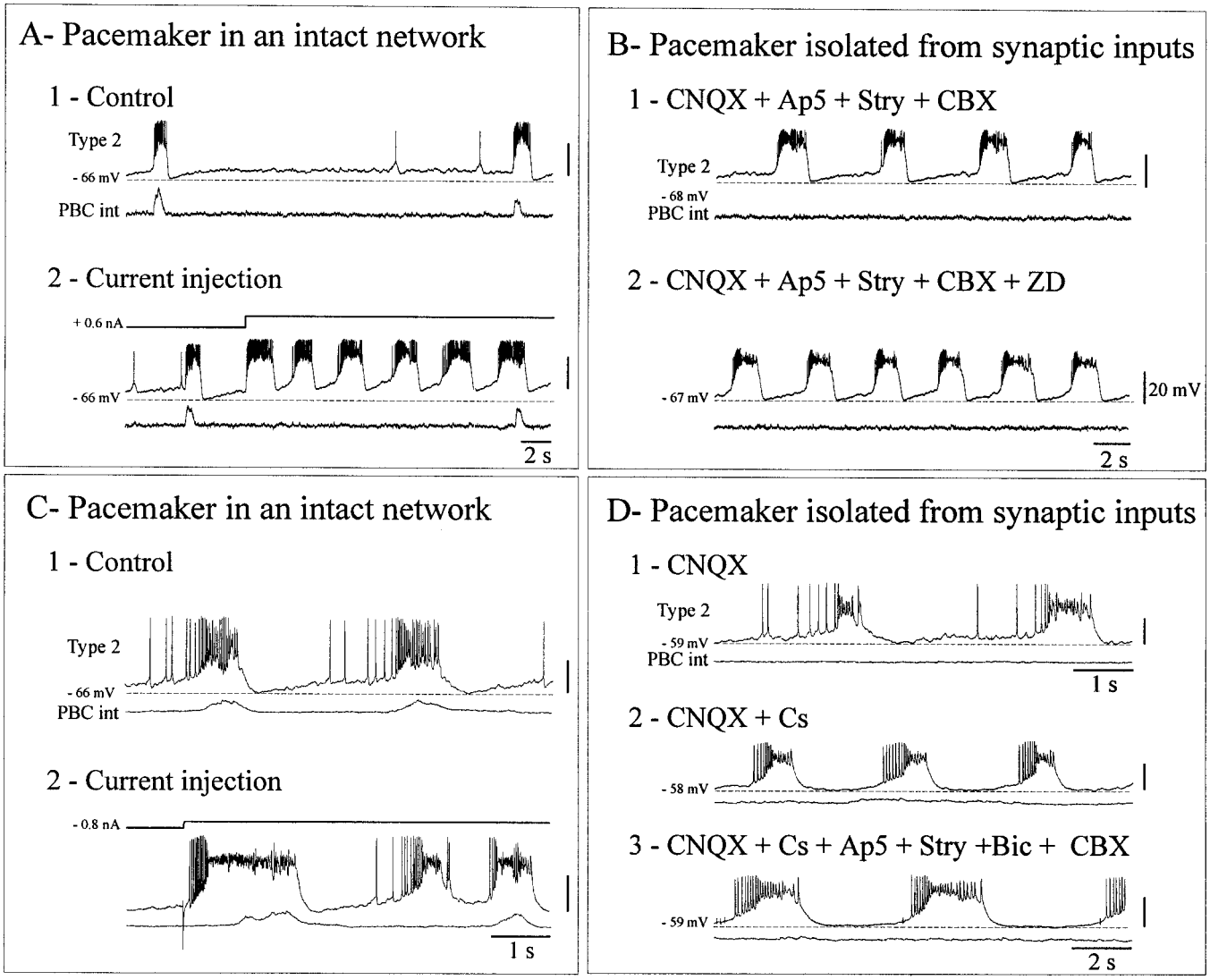

Figure 11. Pacemaker activity in the intact network (*A*, C) and after extensive blockade of synaptic activity (*B*, *D*). A_1, Simultaneous recordings of a type 2 pacemaker neuron (*top trace*) and the population activity (*bottom trace*) under control conditions. A_2, Current injection (*top trace*) induced an increase in the frequency of generated bursts in the neuron (*middle trace*), indicating its pacemaker properties in the intact network. The population activity is unaffected (*bottom trace*). B_1, Recording of the same neuron after synaptic isolation with 20 μM CNQX, 50 μM AP-5, 5 μM strychnine (*Stry*), and 50 μM CBX. B_2, The blockade of the I_h current with ZD 7288 increased the frequency of the rhythmic activity that persisted after synaptic isolation. C_1, Same as A_1. C_2, The release from negative current (*top trace*) induced an increase in the neuron bursting frequency (*middle trace*). The population activity is unaffected (bottom trace). D_1, The neuron remained rhythmically active in 20 μM CNQX. D_2, Its bursting frequency increased after blockade of the I_h current with 5 mM cesium. D_3, The rhythmic activity persisted in 50 μM AP-5, 5 μM strychnine (*Stry*), 20 μM bicuculline (*Bic*), and 50 μM CBX.

(Ramirez et al., 1997, 1998). Under these conditions, the respiratory frequency increases. Like in the absence of the I_h current, the burst amplitude increases only in the motor nucleus, but not in the PBC (Telgkamp and Ramirez, 1999). Thus, in both cases, the XII motor output and the rhythm generator in the PBC were differentially modulated. This is conceptually a very interesting finding, because it has been proposed previously that rhythm generation and motor pattern generation are differentially modulated (Feldman et al., 1990). In the XII motor nucleus, neurons contain a significant amount of I_h current, as shown here and by Bayliss and Berger (1994). Thus, the pronounced amplification of the XII burst amplitude might be the result of a direct modulation of XII motoneurons. It has been demonstrated previously that the induction of bursting properties can be an efficient mechanism to amplify synaptic input (Ramirez and Pearson, 1991), which could also be relevant for the XII nucleus. However, this is only one of many conceivable mechanisms that have to be examined to elucidate the underlying mechanisms. Interestingly, the I_h current undergoes a 10-fold increase during early postnatal development (Bayliss et al., 1994), which correlates with a developmental change in the hypoxic response (Ramirez et al., 1997, 1998).

The dependency of the I_h current on other parameters

Another issue that has to be addressed is the functional relevance of our findings for *in vivo* breathing. One concern is that the frequency of the respiratory rhythm *in vitro* is slower than the breathing rhythm under *in vivo* conditions (~1 Hz) (Smith et al., 1995). This difference could be attributable to the removal of excitatory input and/or to a lower temperature. The frequency difference between *in vivo* and *in vitro* will affect the phase of the

I_h current activation within a respiratory cycle, which in turn might affect the role of the I_h current in respiratory rhythm generation. In our study, we observed that a blockade of the I_h current increased the respiratory frequency over a wide frequency range from 0.07 to 0.7 Hz. However, even at the highest frequency, the *in vitro* rhythm was still slower than the frequency observed in the *in vivo* mouse (~1 Hz). Thus, it is very difficult to predict the physiological role of the I_h current until similar experiments are performed under *in vivo* conditions.

However, of great interest was the finding that the effect of blocking the I_h current was dependent on the initial frequency of the network. At long cycle periods, the blocking effect was more pronounced (178% increase at 0.1 Hz) than at short cycle periods (no more than 100% above 0.15 Hz). The dependency of the I_h current on the cycle period has been described previously for the leech heartbeat system (Olsen and Calabrese, 1996). In this network, the strength of the I_h current increased significantly with longer cycle periods, which should also result in a more pronounced role of the I_h current at lower frequencies. This dynamic property of the I_h current is only one aspect that will be relevant for assessing the functional role of the I_h current in the intact network. The I_h current begins to activate at −50 mV. Therefore, by hyperpolarizing the membrane to more negative values, synaptic inhibitory inputs, calcium-dependent potassium currents, and voltage-dependent potassium currents will play major roles in affecting the activation of the I_h current. In addition, rhythmic fluctuations in intracellular signaling pathways will modulate the activation of the I_h current, which in turn may affect the frequency of the respiratory rhythm (Lüthi and McCormick, 1998, 1999a,b). Thus, it will be an important and interesting task to unravel this complex scenario within the respiratory network, which is particularly promising because of the high percentage of respiratory pacemaker neurons that express an I_h current.

REFERENCES

Angstadt JD, Calabrese RL (1989) A hyperpolarization-activated inward current in heart interneurons of the medicinal leech. J Neurosci 9:2846–2857.

Bal T, McCormick DA (1997) Synchronized oscillations in the inferior olive are controlled by the hyperpolarization-activated cation current I(h). J Neurophysiol 77:3145–3156.

Bayliss DA, Viana F, Bellingham MC, Berger AJ (1994) Characteristics and postnatal development of a hyperpolarization-activated inward current in rat hypoglossal motoneurons *in vitro*. J Neurophysiol 71:119–128.

Berger AJ, Bayliss DA, Bellingham MC, Umemiya M, Viana F (1995) Postnatal development of hypoglossal motoneuron intrinsic properties. Adv Exp Med Biol 381:63–71.

Coggan JS, Purnyn SL, Knoper SR, Kreulen DL (1994) Muscarinic inhibition of two potassium currents in guinea-pig prevertebral neurons: differentiation by extracellular cesium. Neuroscience 59:349–361.

DiFrancesco D, Ferroni A, Mazzanti M, Tromba C (1986) Properties of the hyperpolarizing-activated current (if) in cells isolated from the rabbit sino-atrial node. J Physiol (Lond) 377:61–88.

Feldman JL, Smith JC, Ellenberger HH, Connelly CA, Liu GS, Greer JJ, Lindsay AD, Otto MR (1990) Neurogenesis of respiratory rhythm and pattern: emerging concepts. Am J Physiol 259:R879–R886.

Funk GD, Smith JC, Feldman JL (1994) Development of thyrotropin-releasing hormone and norepinephrine potentiation of inspiratory-related hypoglossal motoneuron discharge in neonatal and juvenile mice *in vitro*. J Neurophysiol 72:2538–2541.

Gasparini S, DiFrancesco D (1997) Action of the hyperpolarization-activated current (Ih) blocker ZD 7288 in hippocampal CA1 neurons. Pflügers Arch 435:99–106.

Golowasch G, Marder E (1992) Ionic current of the lateral pyloric neuron of the stomatogastric ganglion of the crab. J Neurophysiol 67:318–331.

Harris NC, Constanti A (1995) Mechanism of block by ZD 7288 of the hyperpolarization-activated inward rectifying current in guinea pig substantia nigra neurons in vitro. J Neurophysiol 74:2366–2378.

Johnson SM, Smith JC, Funk GD, Feldman JL (1994) Pacemaker behavior of respiratory neurons in medullary slices from neonatal rat. J Neurophysiol 72:2598–2608.

Koshiya N, Guyenet PG (1998) Tonic sympathetic chemoreflex after blockade of respiratory rhythmogenesis in the rat. J Physiol (Lond) 491:859–869.

Koshiya N, Smith JC (1999) Neuronal pacemaker for breathing visualized *in vitro*. Nature 400:360–363.

Lin YJ, Greif GJ, Freedman JE (1996) Permeation and block of dopamine-modulated potassium channels on rat striatal neurons by cesium and barium ions. J Neurophysiol 76:1413–1422.

Lotshaw DP (1997) Effects of K^+ blockers on K^+ channels, membrane potential, and aldosterone secretion in rat adrenal zona glomerula cells. Endocrinology 138:4167–4175.

Lüthi A, McCormick DA (1998) Periodicity of thalamic synchronized oscillations: the role of Ca^{2+}-mediated upregulation of Ih. Neuron 20:553–563.

Lüthi A, McCormick DA (1999a) Ca^{2+}-mediated up-regulation of Ih in the thalamus. Molecular and functional diversity of ion channels and receptors. Ann NY Acad Sci 868:765–769.

Lüthi A, McCormick DA (1999b) Modulation of a pacemaker current through Ca^{2+}-induced stimulation of cAMP production. Nat Neurosci 2:634–641.

Lüthi A, Bal T, McCormick DA (1998) Periodicity of thalamic spindle waves is abolished by ZD 7288, a blocker of Ih. J Neurophysiol 79:3284–3289.

Maccaferri G, McBain CJ (1996) The hyperpolarization-activated current (Ih) and its contribution to pacemaker activity in rat CA1 hippocampal stratum oriens-alveus interneurons. J Physiol (Lond) 497:119–130.

Mayer ML, Westbrook GL (1983) A voltage-clamp analysis of inward (anomalous) rectification in mouse spinal sensory ganglion neurones. J Physiol (Lond) 340:19–45.

McCormick DA, Bal T (1997) Sleep and arousal: thalamocortical mechanisms. Annu Rev Neurosci 20:185–215.

McCormick DA, Pape HC (1990) Properties of a hyperpolarization-activated cation current and its role in rhythmic oscillation in thalamic relay neurons. J Physiol (Lond) 431:291–318.

Neher E (1992) Correction for liquid junction potentials in patch clamp experiments. Methods Enzymol 207:123–131.

Pape HC (1996) Queer current and pacemaker: the hyperpolarization-activated cation current in neurons. Annu Rev Physiol 58:299–327.

Ramirez JM, Pearson KG (1991) Octopaminergic modulation of interneurons in the flight system of the locust. J Neurophysiol 66:1522–1537.

Ramirez JM, Richter DW (1996) The neuronal mechanisms of respiratory rhythm generation. Curr Opin Neurobiol 6:817–825.

Ramirez JM, Quellmalz UJA, Richter DW (1996) Postnatal changes in the mammalian respiratory network as revealed by the transverse brainstem slice preparation of mice. J Physiol (Lond) 491:799–812.

Ramirez JM, Telgkamp P, Elsen FP, Quellmalz UJA, Richter DW (1997) Respiratory rhythm generation in mammals: synaptic and membrane properties. Respir Physiol 110:71–85.

Ramirez JM, Schwarzacher SW, Pierrefiche O, Olivera BM, Richter DW (1998) Selective lesioning of the cat pre-Bötzinger complex *in vivo* eliminates breathing but not gasping. J Physiol (Lond) 507:895–907.

Rekling JC, Feldman JL (1998) PreBötzinger complex and pacemaker neurons: hypothesized site and kernel for respiratory rhythm generation. Annu Rev Physiol 60:385–405.

Rekling JC, Champagnat J, Denavit-Saubie M (1996) Electroresponsive properties and membrane potential trajectories of three types of inspiratory neurons in the newborn mouse brain stem *in vitro*. J Neurophysiol 75:795–810.

Richter DW (1983) Generation and maintenance of the respiratory rhythm. J Exp Biol 100:93–107.

Schwarzacher SW, Smith JC, Richter DW (1995) Pre-Bötzinger complex in the cat. J Neurophysiol 73:1452–1461.

Sharp AA, Skinner FK, Marder E (1996) Mechanisms of oscillation in dynamic clamp constructed two-cell half-center circuits. J Neurophysiol 76:867–883.

Smith JC, Ellenberger HH, Ballanyi K, Richter DW, Feldman JL (1991) Pre-Bötzinger complex: a brainstem region that may generate respiratory rhythm in mammals. Science 254:726–729.

Smith JC, Funk GD, Johnson SM, Feldman JL (1995) Cellular and synaptic mechanisms generating respiratory rhythm: insights from *in vitro* and computational studies. In: Ventral brainstem mechanisms and control of respiration and blood pressure (Trouth CO, Millis R, Kiwull-Schone H, Schlaefke M, eds), pp 463–496. New York: Dekker.

Soltesz I, Lightowler S, Leresche N, Jassik-Gerschenfled D, Pollard CE, Crunelli V (1991) Two inward currents and the transformation of low-frequency oscillations of rat and cat thalamo-cortical cells. J Physiol (Lond) 441:175–197.

Spigelman I, Puil E (1989) K^+ channel blockade in trigeminal root ganglion neurons: effects on membrane outwards currents. J Neurophysiol 62:802–809.

Takahashi T (1990) Inward rectification in neonatal rat spinal motoneurones. J Physiol (Lond) 423:47–62.

Telgkamp P, Ramirez JM (1999) Differential responses of respiratory nuclei to anoxia in rhythmic brainstem slices of mice. J Neurophysiol 82:2163–2170.

Thoby-Brisson M, Telgkamp P, Ramirez JM (1998) Role of the Ih current in respiratory rhythm generation during normoxia and hypoxia. Soc Neurosci Abstr 346:874.

Thoby-Brisson M, Telgkamp P, Ramirez JM (1999) A novel role of the Ih current in regulating the frequency of the respiratory rhythm in mice. Soc Neurosci Abstr 759:1909.

Wischmeyer E, Karshin A (1997) A novel slow hyperpolarization-activated potassium current (IK(SHA)) from a mouse hippocampal cell line. J Physiol (Lond) 504:591–602.